Agricultural and Forest Meteorology 248 (2018) 215–227

Contents lists available at ScienceDirect

Agricultural and Forest Meteorology

journal homepage: www.elsevier.com/locate/agrformet

Monitoring the vegetation activity in China using vegetation health indices

Fengsong Pei[a,*], Changjiang Wu[a], Xiaoping Liu[a,b,**], Xia Li[b], Kuiqi Yang[a], Yi Zhou[a], Kun Wang[a], Li Xu[a], Gengrui Xia[a]

[a] School of Geography, Geomatics and Planning, Jiangsu Normal University, Xuzhou, 221116, PR China
[b] Guangdong Key Laboratory for Urbanization and Geo-simulation, School of Geography and Planning, Sun Yat-sen University, Guangzhou, 510275, PR China

ARTICLE INFO

Keywords:
Vegetation health index
Vegetation condition index
Vegetation activity
China

ABSTRACT

Terrestrial vegetation plays pivotal roles on land-atmosphere interactions, and even global climate change. However, limited attempts have been taken to elucidate the responses of vegetation activity to weather-related drivers (e.g., droughts, floods). This is especially in China with vast area and changeable meteorological conditions. In this paper, the performance of two satellite-based indices, namely vegetation condition index (VCI) and vegetation health index (VHI) were analyzed to detect the vegetation responses to weather-related variations. The dynamics of vegetation activity in China were further examined for the period 1982–2013. We found widely-distributed vegetation stresses in the entire country for a long period (about an average of two months per year) from the VCI and the VHI. In addition, both the two indices indicated increasing vegetation activities over most parts of China during 1982–2013. However, there is no consensus between the two indices at spatial pattern and regional totals. This discrepancy can be due to the negative-correlation assumption of the VHI between the VCI and bright temperature. However, we found that the relationship between the VCI and temperature could be changeable in different regions, especially in China with complex topography, diverse climate conditions and different vegetation types. The findings of this paper highlight the necessity to account for dominant controls on vegetation growth when using the VCI and the VHI to analyze vegetation activity.

1. Introduction

Terrestrial vegetation poses crucial effects on energy budget, water cycle and biogeochemical cycle in ecosystems through vegetation activities (refer to the ability of vegetation interacting with surrounding environments, e.g., photosynthesis, respiration and transpiration) (Piao et al., 2014), and therefore affects earth's climate system (Bala et al., 2007; Peng et al., 2014). In contrast, vegetation activities are sensitive to natural factors (e.g., climate change, atmospheric CO_2 increase and nitrogen deposition) and human disturbances (e.g., afforestation and urban expansion). For instance, vegetation activity was found to be increased through CO_2 concentration increase (Piao et al., 2012), afforestation (Peng et al., 2014) and climate-adaptation (Challinor et al., 2014). However, climatic droughts and urban land development reduced vegetation activity as well (Ji and Peters, 2003; Pei et al., 2013a, 2013b). It is of great concern to monitor the vegetation activity in the scientific community worldwide during past decades.

Satellite data have an advantage in observing a large area to monitor the vegetation activity, in comparison with traditional field-based studies. In past decades, many vegetation indices (VIs) were established to retrieve canopy characteristics to minimize the effect of external factors such as soil background reflectance. Most of the VIs were developed by combining two spectral bands: red and near-infrared band. As a surrogate of vegetation coverage or productivity, the normalized difference vegetation index (NDVI) is one of the widely used VIs to examine vegetation activity at regional to global scales (Fang et al., 2004; Piao et al., 2014). For instances, Peng et al. (2011) evaluated the trends of vegetation growth in China from 1982 to 2010 by using NDVI. Piao et al. (2011) analyzed the relationships between temperature variability and vegetation activity by using the NDVI as a surrogate. de Jong et al. (2011) examined the monotonic greening and browning trends by using global NDVI time-series. Due to weaker short-term signals (i.e., weather-related signals) in a NDVI measurement than long-term ecological one (e.g., soil, topography), the NDVI is difficult to identify vegetation stress to weather anomaly (e.g., droughts) from that of cumulative effects (Kogan, 1995; Seiler et al., 1998). To solve such problems, the vegetation condition index (VCI) was developed to separate the weather-related signals from the ecological one in the NDVI (Kogan and Sullivan, 1993; Seiler et al., 1998). To differentiate the effects of excessive wetness from that of droughts, vegetation health

* Corresponding author at: School of Geography, Geomatics and Planning, Jiangsu Normal University, No.101 Shanghai Road, Tongshan New District, Xuzhou, 221116, PR China.
** Corresponding author at: School of Geography and Planning, Sun Yat sen University, 135 West Xingang RD., Guangzhou, 510275, PR China.
E-mail addresses: fengsong.pei.jsnu@gmail.com, peifs@jsnu.edu.cn (F. Pei), liuxp3@mail.sysu.edu.cn (X. Liu).

http://dx.doi.org/10.1016/j.agrformet.2017.10.001
Received 8 January 2017; Received in revised form 27 July 2017; Accepted 1 October 2017
Available online 07 October 2017
0168-1923/

index (VHI) was further proposed to monitor meteorological droughts by combining the VCI and the hotness of vegetation canopy (Kogan, 1995; Kogan et al., 2011). The VCI and VHI were widely employed and proved effective in evaluating vegetation health and crop production (Kogan 1990; Orlovsky et al., 2011).

As one of vast countries with diverse natural environment, China showed complex trends of vegetation activity due to land-use change and climate fluctuation. For instances, Peng et al. (2011) pointed that the vegetation activity in China increased in the growing season from 1982 to 2010 at the national scale. Lü et al. (2015) found a great spatial heterogeneity of both vegetation greening and browning during 2000–2010. It is still uncertain about trends of vegetation activity in China in past decades, especially vegetation response to changeable conditions (e.g., weather variations). This paper aims to monitor the vegetation activity in China during past decades using two vegetation health indices, the VCI and the VHI over the period 1982–2013. When examining variations of vegetation activity, vegetation index in growing season is often employed as a surrogate of vegetation growth in a whole year. Growing season refers to the period of time in a given year available for plant growth and biomass accumulation. The growing season change is frequently explored by using phenology, satellite data, and surface air temperatures (Linderholm, 2006). The phenological growing season and satellite-based growing season, which are derived from phenology and the NDVI, have significant impacts on competition and fitness of plants, and thus may have profound ecological consequences (Walther et al., 2002). However, for many applications such as monitoring droughts or insect activity, a plant-independent and more general definition are of more interest (e.g., climatological growing season) (Menzel et al., 2003). Chen and Pan (2002) found that mean temperature and growing degree days above 5 degree Celsius (°C) are the most important controls on the beginning and end dates of the growing season in the temperate region of eastern China. Liu et al. (2010) found that the length of growing season is highly correlated with mean temperatures from March to November except in southeast China at the base temperature of 5 °C. A daily temperature of 5 °C for more than 5 days is often used to define growing season (Linderholm, 2006; Song et al., 2010). In this paper, weekly mean temperature of 5 °C was employed to match the growing season length and the composited period of satellite-based images when using the VCI and the VHI (Kogan, 1997). Namely, the growing season in China was spatially identified as when mean temperature in the first (or last) week is above (or below) 5 °C. The VCI and the VHI in the growing season were employed to assess the vegetation activity dynamics in China from 1982 to 2013. The performances of the VCI and the VHI were analyzed and compared from aspects of spatial pattern and regional totals. The trends of vegetation activity dynamics were examined over China from 1982 to 2013 by using least squares fit method.

2. Study area and data processing

2.1. Study area

The study area is located in China, the eastern part of Eurasia continent (Fig. 1). The country spans across multiple climate regimes, including monsoon climate zone across tropical, subtropical and temperate area, temperate continental climate zone and plateau climate zone. The annual average temperature in China varies from above 20 °C in southern China to below −20 °C in Qinghai-Tibetan Plateau. The annual average precipitation ranges from greater than 2400 mm in southern China to less than 100 mm in northwestern China. In addition, the topography in this country is extremely rugged, ranging from −154 m in the Ayding Lake to 8848 m in the Mount Everest in the Qinghai-Tibetan Plateau. Particularly, average elevation in the Qinghai-Tibetan Plateau reaches 4000 m. Because of diverse topography and climate condition, natural vegetation in China contains most of the vegetation types in northern hemisphere from desert and steppe in the arid northwest to the forests in the wet southeast China, and mountain vegetation in the Qinghai-Tibetan Plateau. Since 1978, China experienced an unprecedented urbanization under the economic reform policy. The urbanization brought about dramatic changes in land use and land cover, such as urban land development in Yangtze River delta and Pearl River Delta. In addition, recent climate change also showed important impacts on the vegetation activity in China (Solomon et al., 2007).

2.2. Meteorological data

The gridded meteorological dataset, which covers 32-year period (1982–2013), includes daily mean temperature and daily total precipitation. The dataset was retrieved from the Chinese National Meteorological Information Center/China Meteorological Administration (NMIC/CMA). Specifically, the meteorological datasets were originated from records of 2472 meteorological stations in China. The records were then interpolated to a grid at a resolution of 0.5 × 0.5°. Considering general spatial dependence of meteorological conditions on topography and the complex terrain in China, interpolation was performed by combining thin plate smoothing splines and GTOPO30 elevation data (Hutchinson, 1998; Hong et al., 2005). A cross-validation technique was employed to control the quality of the gridded data. To fit the calculation of the data with other data, the gridded meteorological datasets were reprojected and resampled to a resolution of 4-km, although the data processing did not increase the effective resolution of the datasets.

2.3. Remote sensing data

The vegetation health datasets during 1982–2013, including vegetation condition index (VCI) and vegetation health index (VHI) data at a resolution of 4-km, were derived from the Center for Satellite Applications and Research (STAR) from the National Oceanic and Atmospheric Administration (NOAA). These datasets were produced from the Global Area Coverage (GAC) dataset observed by the Advanced Very High Resolution Radiometer (AVHRR) onboard the NOAA-7, 9, 11, 14, 16 and 18 with afternoon orbits. Daily records from the satellite observation were aggregated to a seven-day period by using the AVHRR GAC Level 1B dataset (Kogan et al., 2011). The average values of the VCI and the VHI in the growing season were then calculated as a surrogate of annual vegetation health when analyzing the vegetation activities. Because of the morning satellite orbits from September 1994 to February 1995, both the VCI and VHI data were not available. For ensuring the continuity, the missing data were substituted using average values of the VCI and the VHI of the corresponding records before and after the year 1994.

Monthly NDVI images at 1 km resolution in 2013 were obtained from MODIS product (MOD13) to mask nonvegetated area in China. In addition, land cover type data at annual scale were also obtained from MODIS L3 product (MCD12). Both the MOD13 and MCD12 data were downloaded from the Earth Observing System Data Gateway at the Land Processes Distributed Archive Center (http://lpdaac.usgs.gov/). All the images were then aggregated to a resolution of 4 km × 4 km. In addition, the method of maximum value composite (MVC) was conducted to obtain annual NDVI. Furthermore, the pixels with average NDVI less than 0.1 were marked as non-vegetated area.

2.4. Crop production records from statistical yearbook

The crop production data, including yields of rice, wheat, maize, soybean and millet, were collected at provincial level over the period of 1982–2013 from China Statistical Yearbook. The China Statistical Yearbook was compiled by State Statistical Bureau, People's Republic of China. A total of 30 provinces were selected excluding Hainan Province and Chongqin City because of some missing records in the two regions.

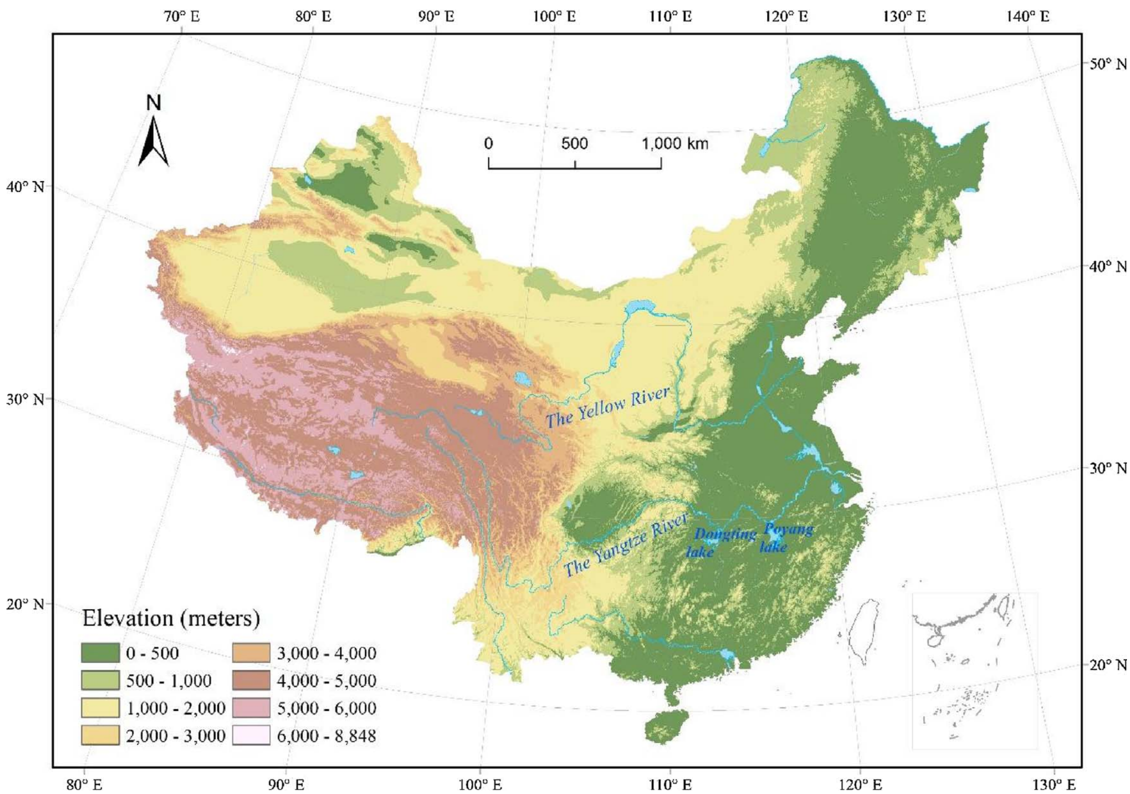

Fig. 1. Location of the study area.

2.5. Palmer drought severity index (PDSI) data

Monthly Palmer Drought Severity Index (PDSI) data from 1982 to 2013 (Dai et al., 2004) were obtained from the National Center for Atmospheric Research (NCAR) (http://www.cgd.ucar.edu/cas/catalog/climind/pdsi.html). The PDSI data were computed by using observed or model monthly surface air temperature and precipitation, plus other surface forcing data (Dai et al., 2004). To keep consistency with the VCI and the VHI data, the monthly PDSI data were further aggregated to annual scale using the growing season mean values.

3. Methods

3.1. Vegetation health indices

The NDVI is a remote-sensed indicator to measure photosynthetic activity of vegetation. Thus, The NDVI is frequently employed as a proxy of plant greenness or vegetation growth (Liu and Gong, 2012; Piao et al., 2014). In detail, the NDVI is calculated as the normalized ratio of the near-infrared band and visible band from remote-sensed images:

$$\mathrm{NDVI} = (\mathrm{NIR} - \mathrm{RED})/(\mathrm{NIR} + \mathrm{RED}) \quad (1)$$

where NIR and RED stand for the spectral reflectance measurements acquired in the visible (red) and near-infrared bands of remote-sensed images, respectively. This index varies between −1.0 and +1.0, despite no ecological meaning when less than zero. Generally, high NDVI indicates a favorable condition for vegetation growth, which associated with highly photosynthetically active vegetation. In contrary, a low NDVI means little difference between the red and near-infrared radiation recorded by the satellite sensor. This happens when there is little photosynthetic activity, or when there is just very little near-infrared radiation (e.g., vegetation that is dead or stressed).

As one of the most commonly used vegetation indices, the NDVI are often associated with changeable meteorological condition (e.g., droughts, floods) and cumulative effects of local resource background (e.g., soil, topography and vegetation type) (Kogan, 1990), especially in areas with a large number of different vegetation covers such as in China. For better capturing the dynamics of vegetation activity across China, it is essential to separate the vegetation activity anomalies that caused by changeable meteorological factors from the ecological effects of local drivers in the NDVI. Kogan (1995) found that smoothing technology could make the difference among time series of NDVI more apparent when monitoring weather-related variation. Thus, vegetation condition index (VCI) was further developed by scaling smoothed weekly NDVI values relative to the amplitude of their ranges when archived data is available, to separate weather-related signal in the NDVI from ecological resource background (Kogan and Sullivan, 1993; Kogan, 1995). To match the periods of 3–7 days for morphological changes and leaf appearances (Ulanova, 1975) and the periods of 3–5 days for weather patterns change, one week's temporal aggregation of satellite data was selected when developing the VCI (Kogan, 1997). The VCI is defined as follows:

$$VCI = 100*(NDVI - NDVI_{\min})/(NDVI_{\max} - NDVI_{\min}) \quad (2)$$

where $NDVI$, $NDVI_{\max}$ and $NDVI_{\min}$ represent the smoothed weekly NDVI, their absolute maximum and minimum values in a given period, respectively. The VCI was used as one of the important vegetation indicators when monitoring weather-related variations, such as droughts. On the condition of excessive soil wetness and/or long cloudiness, the NDVI is normally very depressed and the VCI has low values which can be interpreted erroneously as a drought event. For distinguishing droughts from excessive soil wetness and/or long cloudiness, VHI was developed through a combination of VCI and temperature condition index (TCI) (Kogan, 1995; Kogan et al., 2011):

$$VHI = a*VCI + (1 - a)*TCI \quad (3)$$

$$TCI = 100*(BT_{\max} - BT)/(BT_{\max} - BT_{\min}) \quad (4)$$

where the TCI reflects the stress of temperature; the BT defines

brightness temperatures; a is a coefficient to quantify the relative contributions of moisture and temperature to the vegetation health; BT, $BT_{\max}$ and $BT_{\min}$ represent the smoothed weekly BT, the absolute maximum and minimum of the BT, respectively. Since the contributions of moisture and temperature to vegetation health are unknown for a specific location at some periods, the proportion was often assumed equal for simplicity (i.e., $a = 0.5$). The detailed description of this algorithm can be found in the study of Kogan et al. (2011).

As shown in Eqs. (2)-(4), vegetation health indices (VHs), including VCI, TCI and VHI, vary between 0 (extreme stress) and 100 (most favorable condition), with the VHs between 40 and 60 reflecting normal vegetation condition (Kogan et al., 2011). A decrease in the VHs from 40 to 0 indicates intensification of vegetation stress. In contrary, VHs increase from 60 to 100 suggests improvement of vegetation condition. In this paper, we evaluated the vegetation condition at different categories by identifying the VHs in three ranges: (1) in stress (0–40); (2) in normal condition (40–60) and (3) in favorable condition (60–100).

3.2. Least squares fit method to analyze the trends of vegetation activity

While analyzing the dynamics of vegetation activity, time series of VCI and VHI data in the growing season in China was analyzed from 1982 to 2013. To match the temporal aggregation of satellite data and growing season length, weekly mean temperature of 5 °C was employed as a threshold of growing season when monitoring dynamics of vegetation activity in China by using the VCI and the VHI. Both the spatial patterns and the regional totals of average VCI and average VHI in the growing season were calculated to reflect the dynamics of vegetation activity. The trends of the VCI and the VHI were examined using least squares fit method. The analyses were performed as follows: (1) identify start and end time of the growing season at cell scale by using weekly mean temperature from 1982 to 2013; (2) calculate the average VCI and VHI in the growing season as an annual surrogate of vegetation growth in past decades; (3) examine the interannual trends of the VCI and the VHI by using a simple least squares fit method. The linear trends of the VCI and the VHI were calculated as follows:

$$VH_t = a + b\,t + e_t \tag{5}$$

where VH_t is the pixel value (or the mean in the whole country) of the VHI and the VCI at year T from 1982 to 2013; e_t is a disturbance (residual) term with mean value of zero. The regression coefficient b gives the trends of the VCI and the VHI per decade. By using Eq. (5), the trends of vegetation activity was examined from both spatial pattern and regional totals.

3.3. Performance assessment of vegetation health indices for monitoring vegetation activity

The vegetation health indices, including both the VCI and the VHI, were widely employed in monitoring vegetation stress, crop production and biomass estimation (Unganai and Kogan, 1998; Kogan et al., 2005; Orlovsky et al., 2011). As shown in Eq. (3) (a = 0.5), the VHI assumes a negative-correlation between VCI and brightness temperature when representing vegetation activity (Karnieli et al., 2006). The performances of the VCI and the VHI on monitoring vegetation activity were further compared and evaluated by: (1) validating the two indices with crop production data from statistical yearbooks; (2) checking the consistency between the two indices with the PDSI data; (3) examining negative-correlation assumption of the VHI between the VCI and temperature by dry-wet zones and vegetation types.

When monitoring vegetation activity, weather-related impacts (e.g., droughts) are usually first apparent in agriculture (Komuscu, 1999; Bhuiyan et al., 2006). Thus, suitability of the VCI and the VHI on representing the vegetation activity was validated by using crop production records from statistical yearbook. In this paper, the crop production data were collected at provincial level. In particular, the records from four provinces in main crop producing area in China were selected, including Shandong and Anhui Province Province from Huang-Huai-Hai Plain, Jiangxi Province from Poyang Lake Plain and Hunan Province in Dongting Lake Plain.

In addition, we compared the spatial pattern of the VCI and the VHI with that of the PDSI. The PDSI were widely employed in reflecting droughts, soil moisture, and so on (Szép et al., 2005; Trenberth et al., 2014). Thus, performances of the VCI and the VHI were evaluated by using the PDSI as a comparison. The PDSI data from Dai et al. (2004) were found effective in capturing both surface moisture conditions and stream flow. However, considering differences of the time-scale between the PDSI and the VCI/VHI, the PDSI data were compiled from monthly to annual scale by using the growing season PDSI as a surrogate.

Finally, negative-correlation assumption between the VCI and bright temperature was examined to assess dynamics of vegetation activity by using China as an instance. To ascertain data precision and match the vegetation growth estimates, temperature measurements from meteorological stations were employed as a surrogate of bright temperature, instead. The spatial pattern of the correlation between the VCI and temperature was then analyzed by dry-wet zones and vegetation types. In this paper, three zones in China that span much of the climate conditions: humid, semi-humid and semi-arid, and arid regions (Fig. 7c) was distinguished. The dry-wet schema was roughly based on the work of Huang (1958) and the committee on natural division of the Chinese Academy of Sciences (1959), followed by a recombination of these climate zones.

3.4. Dynamics of vegetation activity in China

To explore the dynamics of vegetation activity, the VCI and the VHI in the growing season were employed from 1982 to 2013. In detail, non-vegetated area in China was firstly identified and masked using NDVI images. Interannual temperature anomaly of the VCI and the VHI (deviation from the long-term means) in the growing season were calculated in China from 1982 to 2013. Average VCI and VHI were calculated for the full range (0–100) to examine average vegetation condition in China in past decades. For further analyzing the changes of the VCI and the VHI, average VCI and VHI were also obtained at the ranges of 0–40, 40–60 and 60–100, respectively. Some specific anomalies of vegetation activity were examined for the period 1982–2013 as well. The VCI and the VHI were analyzed and compared at both the spatial pattern and regional totals for the period 1982–2013.

Furthermore, we analyzed the probable causes and factors affecting the differences between the VCI and the VHI. Simple correlation analyses were conducted both temporally and spatially to examine the negative-correlation assumption between vegetation growth and the temperature. Trends of the VCI, the VHI and temperature anomalies in the growing season were calculated by using a pixel-to-pixel regression analysis (i.e., simple least squares fit in Eq. (5)).

4. Results and discussions

4.1. Average growing-season length in China

Growing season length in China was derived as the time range when weekly average temperature exceeded 5 °C in the first and last week over the period 1982–2013. As shown in Fig. 2, growing season length showed an increasing trend from northern to southern China. In detail, it varied from up to 52 weeks in southern China to 21–30 weeks in north-eastern China. It should be noted that the growing-season length was found to be shortest in Qinghai-Tibetan Plateau where heat energy is the dominant factor affecting vegetation growth (less than 10 weeks). Such short growing-season could be associated with the high elevation of more than 4000 m in this area. These results are in accordance with

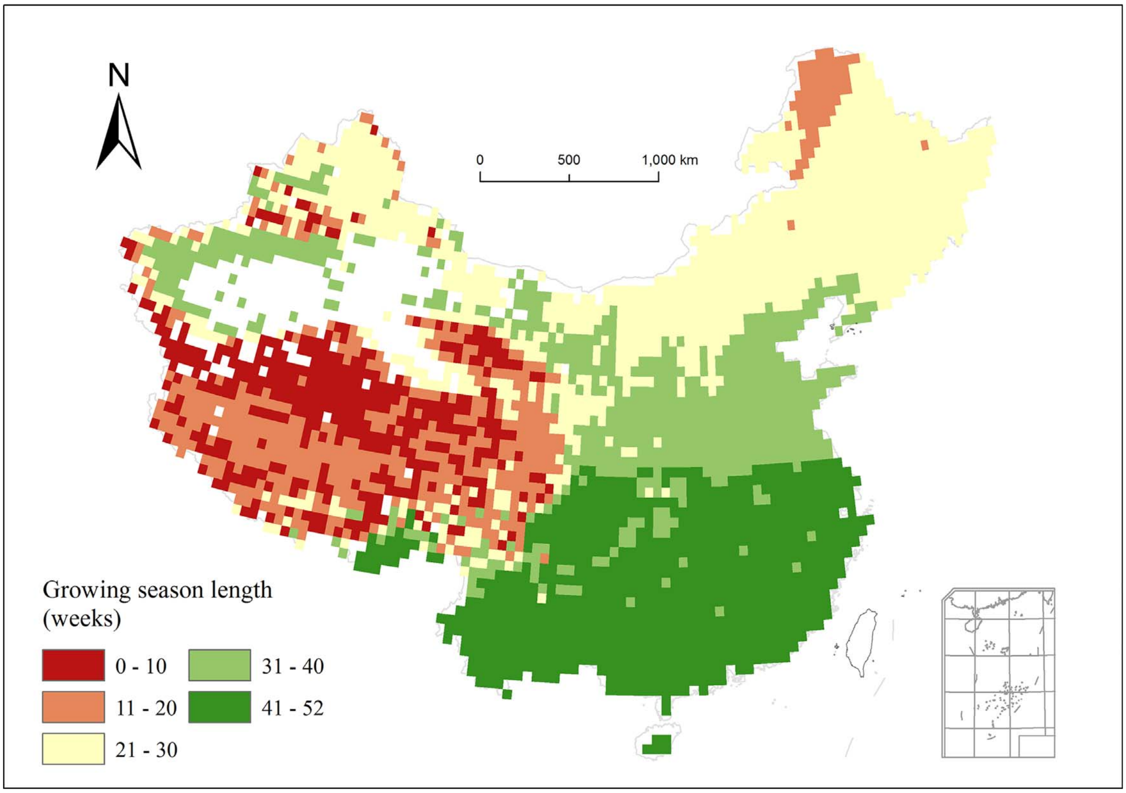

Fig. 2. Spatial distribution of growing season length in China.

the findings of Song et al. (2010), who examining the changes of growing season using five different indices.

4.2. Changes in the VCI and the VHI

A full range analysis (0–100) of the VCI and the VHI was firstly analyzed to detect average vegetation condition in China. As shown in Figs. 3–5, differences could be found between the VCI and the VHI regarding total amounts and spatial patterns. Take China as a whole, average VCI in the growing season was 51 ± 8 over the period 1982–2013, in comparison with the average VHI of 48 ± 4 (Fig. 3a and b). This result indicates a normal condition of the vegetation growth at national scale. In addition, both the VCI and the VHI showed increasing trends in past decades. As shown in Fig. 3a, the increasing rate of the growing-season VCI during 1982–2013 reached 6.27 per decade (R2 = 0.491, P = 0.000), and 0.86 per decade (R2 = 0.032, P = 0.324) for the VHI (Fig. 3b). This difference could be associated with the offset of the VCI by the brightness temperatures (Eqs. (3) and (4)). Despite the increase in the past 30 years, the trends showed a decrease in comparison to that of the 1982–1999 with the increasing rate of 7.11 and 1.96 per decade for the VCI and the VHI, respectively. The results were consistent with the results from the satellite-derived NDVI analysis (Peng et al., 2011).

Besides full range analysis, the VCI and the VHI were also analyzed for different ranges, including 0–40, 40–60 and 60–100. As shown in Fig. 3c, obvious vegetation stress in 1982–1983 was identified in China by using the VCI as indicator (0–40). This phenomenon was associated with the wide distribution of vegetation growth that is in stress, which caused by the climate anomaly (i.e., floods) during the 1982–1983 El Niño events (Zhai et al., 1999; Wang et al., 2003). However, the vegetation stress in this period, which was derived from the VHI, was less severe at the national scale (Fig. 3d), indicating a limited ability of the VHI in capturing the floods-induced stress on vegetation growth. In addition, relatively severe vegetation stresses in 1986, 1989, 1995–1996, were identified at national scale by both the VCI and the VHI. Such vegetation conditions could be associated with the widespread occurrences of dry area in China (Zou et al., 2005). In particular, an obvious vegetation stress could be found in 2000 based on the VCI, associating with the severe droughts occurred in this period across the country (Wang et al., 2003). Similar low values could also be observed at other ranges (e.g., 40–60 and 60–100) in these periods by using the VCI and the VHI (Figs. 3e–3h). The results proved the vegetation stresses in the period of 1982–1983, 1986, 1989, 1995–1996 and 2000. All these results indicated the large-scale anomalies of vegetation activity in these periods over entire China.

The spatial pattern of vegetation condition and its duration in China was also examined using growing-season VCI and VHI at the ranges of 0–40, 40–60 and 60–100, respectively. As shown in Figs. 4a and 4b, average VCI between 0 and 40 in the growing season was 24 at a duration of 9 weeks in the whole China, in comparison with 31 for the VHI at 8 weeks (Figs. 5a and 5b). The results indicated a widely-distributed vegetation stress for a long period (about two months) in this country from both the VCI and the VHI. In addition, observed normal and favorable vegetation condition could be different by using VCI or VHI as indicators. In detail, average VCI between 60 and 100 in the growing season was 76 at a duration of 10 weeks (Figs. 4e and 4f), in comparison with 68 for the VHI at 5 weeks (Figs. 5e and 5f). Furthermore, average VCI between 40 and 60 in the growing season was 50 at a duration of 6 weeks (Figs. 4c and 4d), in comparison with 50 for the VHI at 13 weeks (Figs. 5c and 5d). The results indicated a rare occurrence of normal vegetation condition and more occurrences of favorable vegetation condition by using the VCI as an indicator. However, this result is reversed according to the VHI. A widely normal vegetation condition was observed in China from the VHI in past decades.

4.3. Performance assessment of the VCI and the VHI on detecting vegetation activity

4.3.1. Validation of the VCI and the VHI with crop production data

According to country-level analysis, the correlations between crop

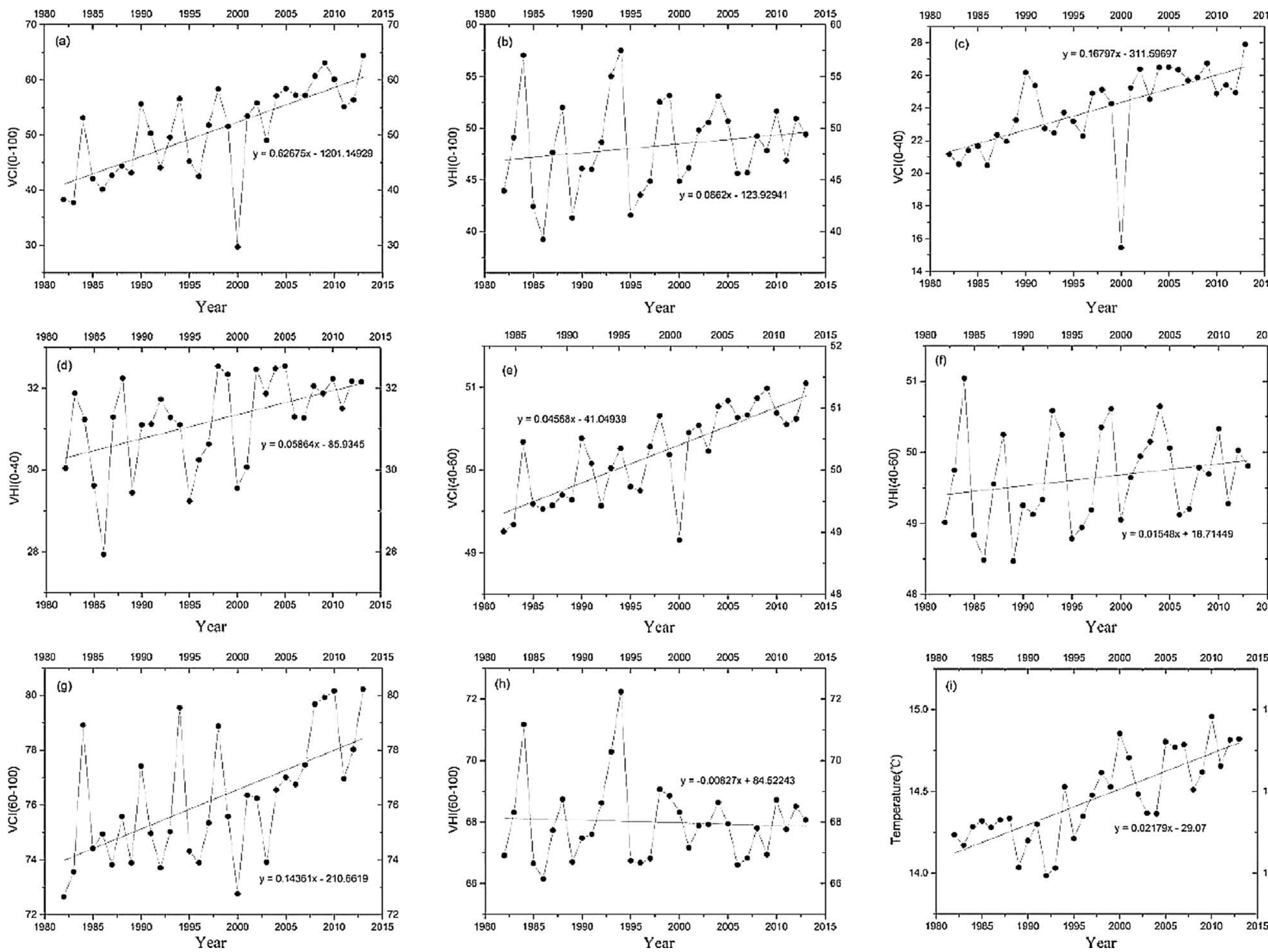

Fig. 3. Interannual variations of VCI, VHI and temperature in China from 1982 to 2013. (a) the VCI at the ranges of 0–100, (b) the VHI at the ranges of 0–100, (c) the VCI at the ranges of 0–40, (d) the VHI at the ranges of 0–40, (e) the VCI at the ranges of 40–60, (f) the VHI at the ranges of 40–60, (g) the VCI at the ranges of 60–100, (h) the VHI at the ranges of 60–100, (i) temperature change.

production and the VCI are significant for 20 of the 29 provinces in China ($P < 0.05$). However, there are only 13 provinces with the correlations significant for the VHI. Particularly, a total of 4 provinces, which is from main crop producing area in China, were selected and analyzed. Firstly, Shandong Province, which is located in semi-humid regions in China with negative correlation between the VCI and temperature, was analyzed (Figs. 6 a and 7). We found that the correlation was significant between crop production and the VCI ($R = 0.40$; $N = 28$; $P = 0.020$) or the VHI ($R = 0.50$; $N = 28$; $P = 0.000$) in this province.

Secondly, three provinces, including Anhui, Jiangxi and Hunan in humid regions with positive correlation between the VCI and temperature, were analyzed as well (Fig. 7). As shown in Fig. 6b, a significant correlation could be found between crop production and the VCI ($R = 0.64$; $N = 28$; $P = 0.000$), or the VHI ($R = 0.55$; $N = 28$; $P = 0.001$) in Anhui Province in the Huang-Huai-Hai Plain. It is similar in Jiangxi Province in the Poyang Lake Plain for the VCI ($R = 0.62$; $N = 28$; $P = 0.000$) and the VHI ($R = 0.50$; $N = 28$; $P = 0.004$) (Fig. 6c), and in Hunan Province in the Dongting Lake Plain for the VCI ($R = 0.49$; $N = 28$; $P = 0.005$) and the VHI ($R = 0.28$; $N = 28$; $P = 0.122$) (Fig. 6d). The results indicated that the performances of the VCI and the VHI could be associated with climatic conditions.

4.3.2. Relationships between vegetation health indices and temperature changes

To distinguish causes of the difference between the VCI and the VHI when monitoring vegetation activity, we examined the relationships between VCI, VHI and temperature changes. We found that temperature shows an increase at national scale during 1982–2013, at a rate of 0.22 °C/decade ($R2 = 0.73$, $P < 0.001$) (Fig. 11). Based on statistical analysis, temporal variations of the VCI corresponded closely with the raised temperature in this period ($R = 0.501$; $P = 0.003$; $N = 32$) (Figs. 3a and 3i). Despite the significant correlation between VCI and temperature, a weaker correlation was found between the VHI and the temperature in China ($R = 0.456$; $P = 0.009$; $N = 32$) (Figs. 3b and 3i). This discrepancy could be associated with the negative-correlation assumption of the VHI between vegetation growth and brightness temperature (Eq. (3) and (4)). However, relationships between vegetation growth and temperature could be changeable in different ecosystems (Karnieli et al., 2006). As shown in Fig. 7, an obvious negative correlation could be found in the northern China, where precipitation is the main constraints. However, the correlation is positive in the southern China and eastern Qinghai-Tibetan Plateau. In the southern China, plant growth could be enhanced with the concurrent increase of temperatures and precipitation (Peng et al., 2011). In the eastern Qinghai-Tibetan Plateau, warming temperature in past decades could extend the growing season and therefore enhanced the vegetation photosynthesis, particularly in the regions where water is non-limiting (Xiao and Moody, 2004). Consequently, this phenomenon could lead to artificial vegetation health of the VHI in southern China or eastern Qinghai-Tibetan Plateau when monitoring vegetation activity.

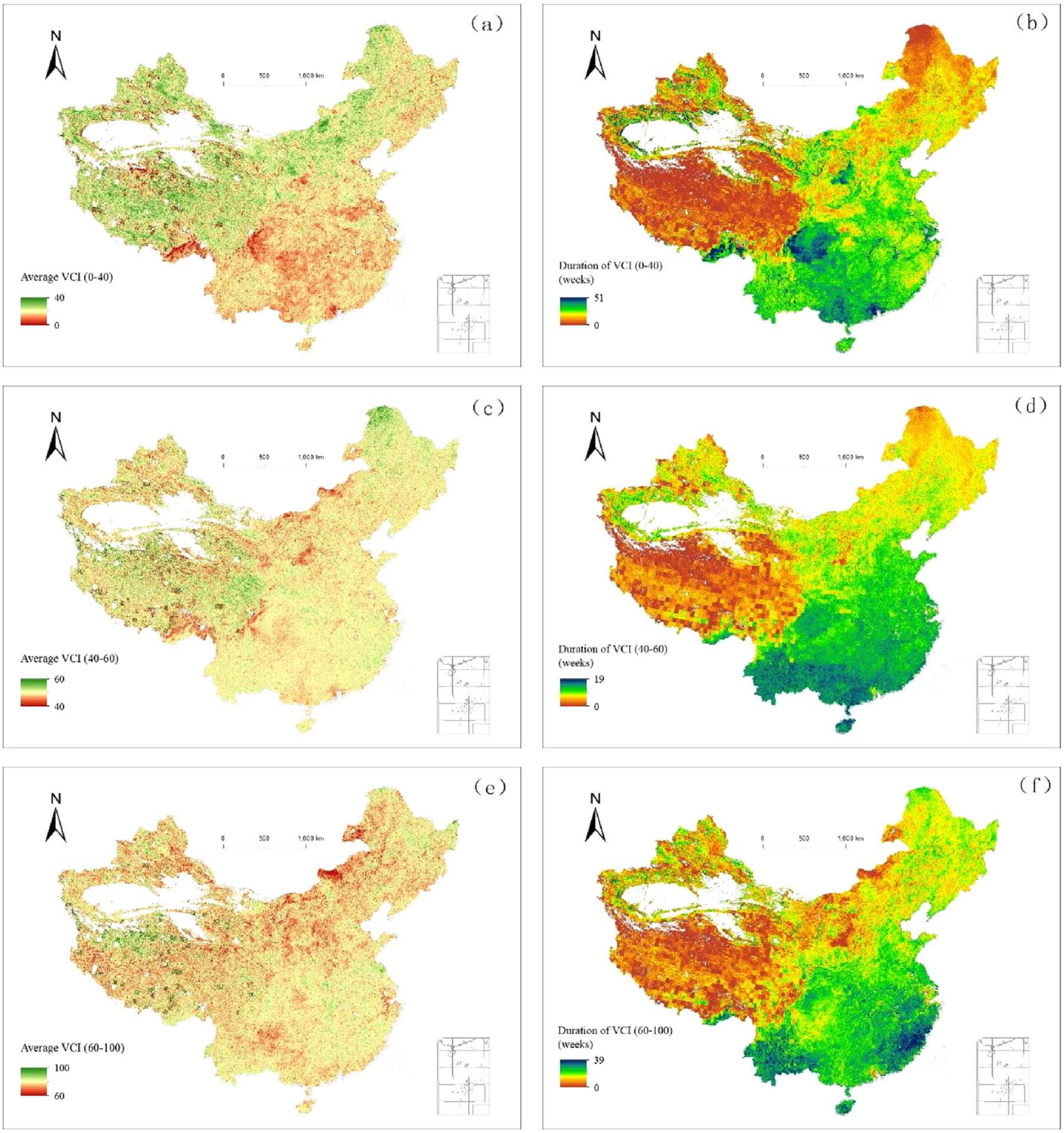

Fig. 4. Average values and its corresponding duration of the VCI and temperature changes in China during 1982–2013. (a) average VCI between 0 and 40 and, (b) its corresponding duration, (c) average VCI between 40 and 60 and, (d) its corresponding duration, (e) average VCI between 60 and 100 and, (f) its corresponding duration.

4.3.3. Relationships between vegetation health indices and palmer drought severity index (PDSI)

The performances of the VCI and the VHI were also explored by comparing the spatial pattern of the two indices with that of the PDSI. As shown in Fig. 5c, an obvious vegetation stress in the northern China was observed using the VHI as an indicator. This vegetation stress could be associated with the droughts occurred in this region (Fig. 8). However, vegetation stress in this region was weaker from the VCI than the VHI (Figs. 4c and 5c). In addition, vegetation stress in the southern China (Fig. 8) was more obvious from the VCI than that from the VHI (Figs. 4c and 5c). The spatial differentiation could be associated with the introduction of the TCI when using the VHI as an indicator. That is, the VHI could be more effective than the VCI in the northern China because of the negative correlations between the VCI and temperature (Fig. 7). In contrary, the positive correlations led the weaker performance of the VHI than the VCI in the southern China (Figs. 4c, 5c and 7).

4.3.4. Vegetation-type-based analysis of the relationships between the VCI and temperature changes

For examining the assumption of the VHI that vegetation growth is negatively correlated with brightness temperature, simple correlation analysis between the VCI and temperature was conducted spatially across China by using time-series of data during 1982–2013. The spatial heterogeneities of the correlations were further analyzed by dry-wet zones and vegetation types (e.g., grass, crop, forest). As shown in Fig. 7, negative correlations between the two factors are obvious in the grassland in semi-arid and sub-humid climatic regions (e.g., eastern Inner Mongolia) where precipitation is the main limiting factor for vegetation growth (Pei et al., 2013b). In these regions, increased temperature showed vegetation stress in the condition of drought occurrence (Figs. 8 and 11). This effect is in accordance with changes of the VCI (Fig. 9b). Thus, the VHI produced similar results with the VCI (Fig. 10b), indicating the good performance of the VHI when detecting the vegetation activity in such regions.

Despite these negative correlations, it showed positive correlations

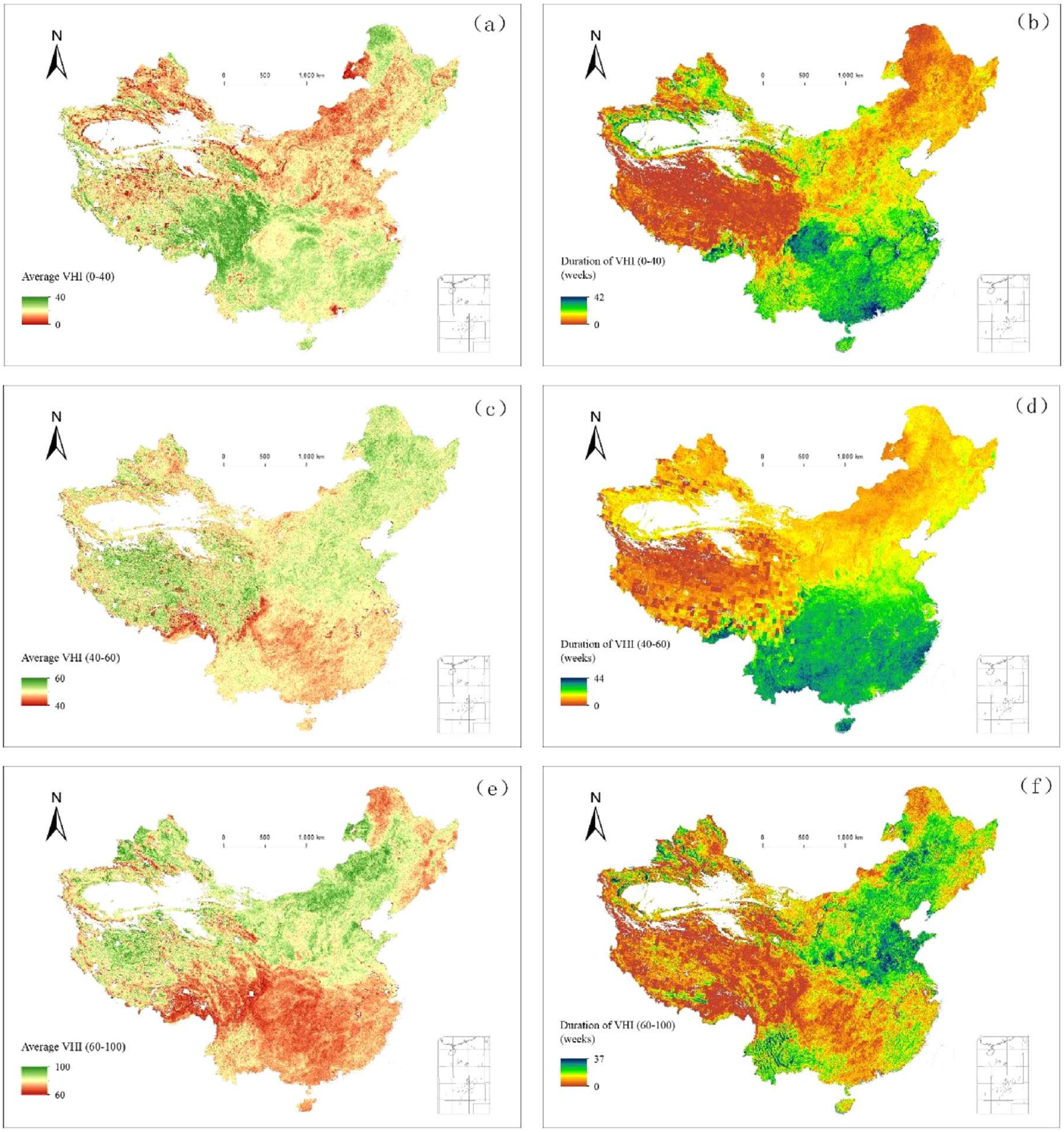

Fig. 5. The same details as Fig. 4, but for the VHI.

in the evergreen needleleaf trees, evergreen broadleaf trees, deciduous broadleaf trees and shrub in the southern China with humid monsoon climatic condition (Fig. 7). In such regions, plant growth could be enhanced with the concurrent increase of temperatures and precipitation (Peng et al., 2011). This change could be opposite to the assumption of negative-correlations between the VCI and temperature. Thus, the VHI could be limited for probably underestimating the stress when identifying the vegetation activity.

Furthermore, it should be noted that the VHI shows obvious decreases in the eastern Qinghai-Tibetan Plateau, in contrast to the weak effects of the VCI (Figs. 9b and 10b). This phenomenon could be caused by the increasing temperature in this region during past decades (Fig. 11). As shown in Fig. 7, obvious positive correlations could been found over large area in the Qinghai-Tibetan Plateau. In particular, in the eastern Qinghai-Tibetan Plateau with an average elevation of more than 4000 m, similar to the high latitudes, heat energy is the dominant control on vegetation growth. The warming climate could provide a favorable condition to vegetation growth (Figs. 7 and 11). This result is consistent with the findings that the NPP in this region witnessed some increases during past decades (Zhao and Running, 2010). Consequently, vegetation stress could be overestimated by the VHI in the east Qinghai-Tibetan Plateau. These results are in accordance with Karnieli et al. (2006, 2010)'s findings concerning the limit of the VHI when employing in high latitude regions. Thus, we propose that the VCI and the VHI should be used cautiously in the context of climate warming, especially in the eastern Qinghai-Tibetan Plateau with an average elevation of more than 4000 m.

4.4. *Trends of vegetation activity in China from 1982 to 2013*

To examine the trends of vegetation activity in past decades, data ranges, mean values of the linear trends of the VCI and the VHI in the growing-season in China were further analyzed for the period 1982–2013. As shown in Figs. 9a and 10a, average VCI in the growing season were within the ranges of 18–84, in comparison with the VHI between 11 and 79. In addition, regional average values of the VCI and the VHI reached 51 ± 6 and 48 ± 5, respectively. Furthermore, the VCI revealed an overall increasing trend of 6.28 ± 8.33 per decade.

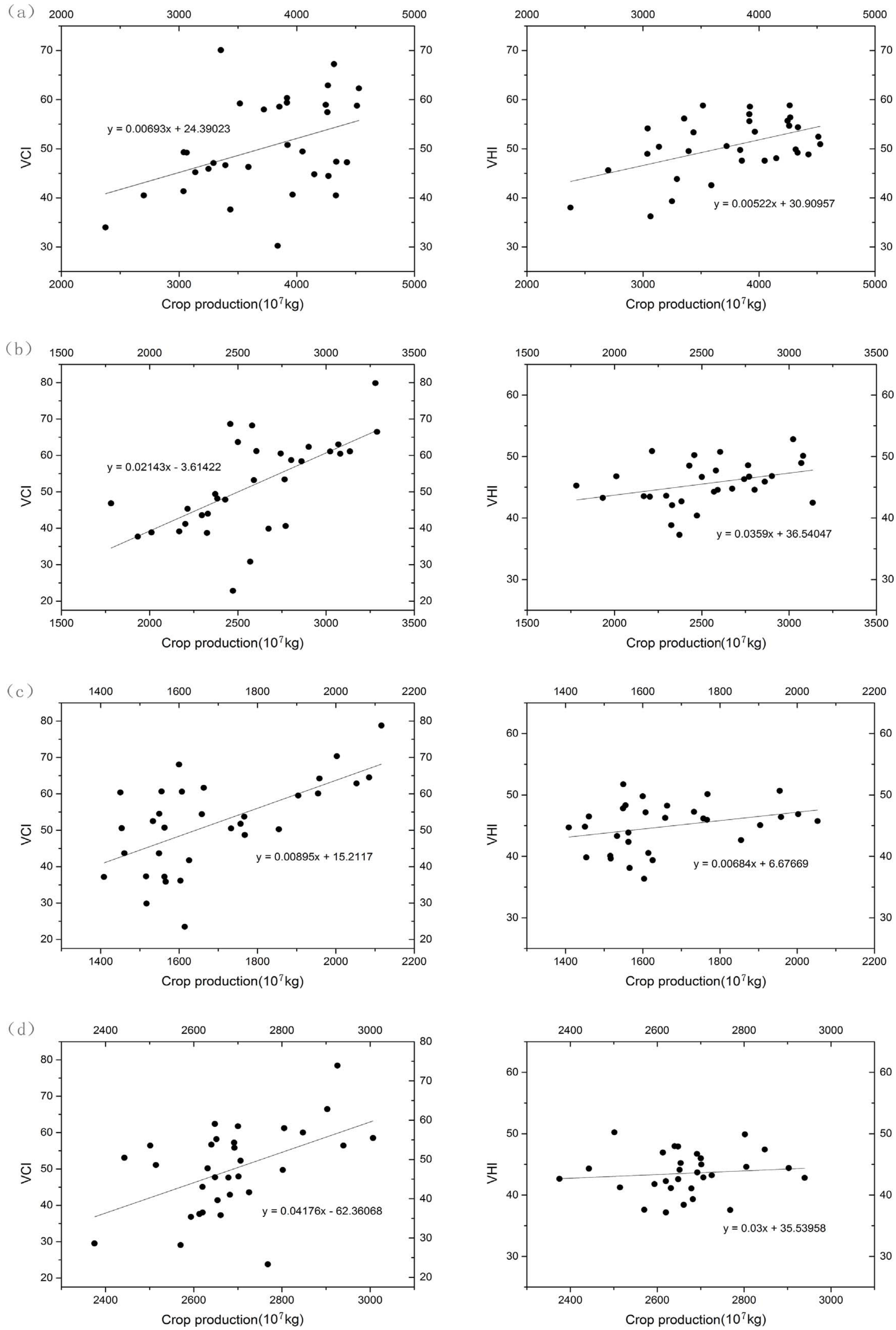

Fig. 6. Correlations between the VCI, the VHI and crop production in: (a) Shandong Province in Huang-Huai-Hai Plain, (b) Anhui Province in Huang-Huai-Hai Plain, (c) Jiangxi Province in Poyang Lake Plain, (d) Hunan Province in Dongting Lake Plain.

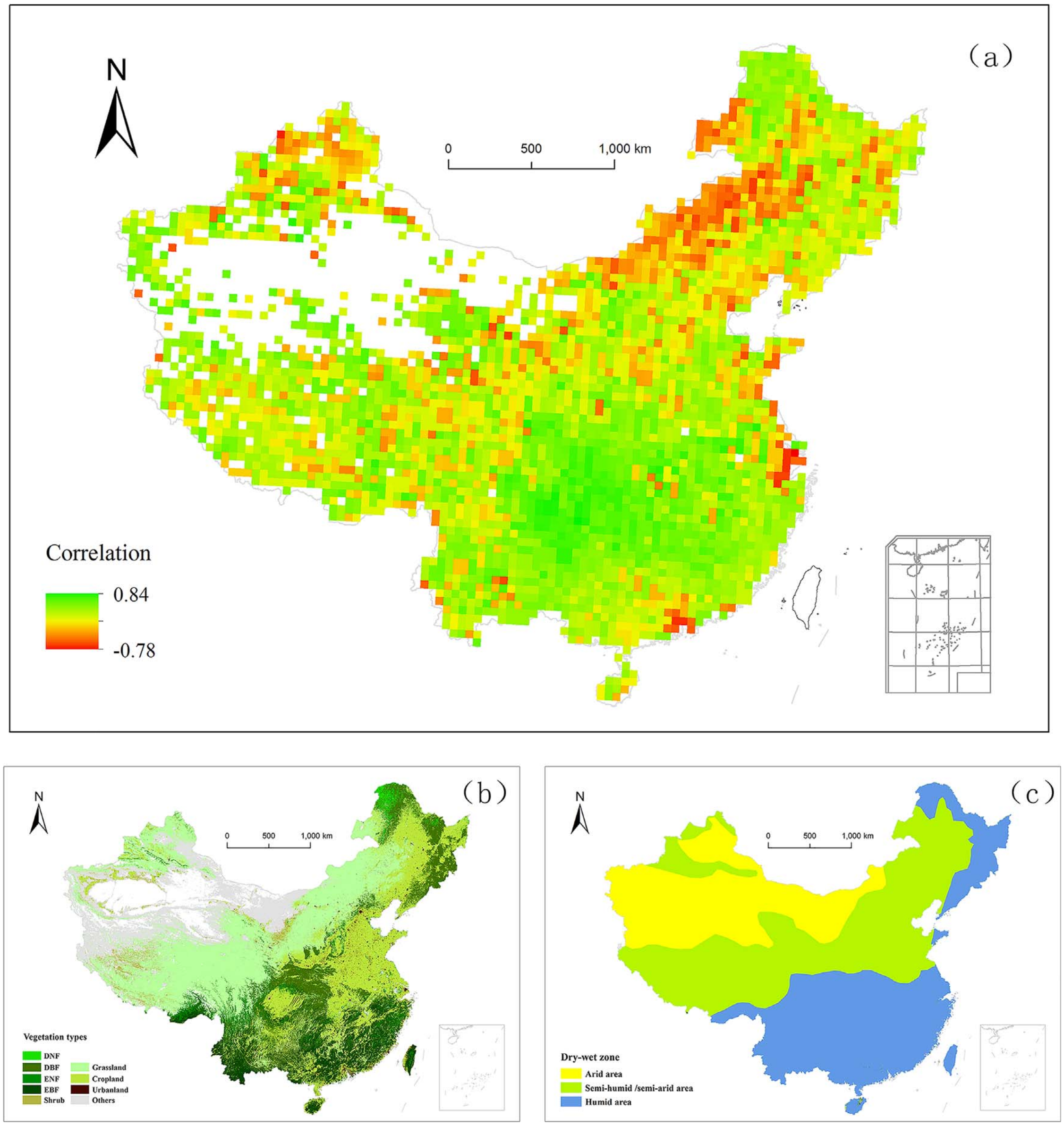

Fig. 7. Statistical relationship between VCI and temperature, distribution of vegetation types and dry-wet zones in China: (a) correlations, (b) vegetation types, (c) dry-wet zones.

However, the VHI showed an increase of 0.81 ± 5.39 per decade (Figs. 9 b and 10b).

Spatially, our results showed that about 78% of the area in China show a positive trend from the VCI, and 60% based on the VHI (Figs. 9b and 10b). This result indicates that vegetation growth can be enhanced in most of the regions in China from both the VCI and the VHI. For instances, vegetation activity in southern China could be enhanced in the condition of concurrent increase of temperature and precipitation (Peng et al., 2011). The results are also consistent with the findings of Piao et al. (2009), who found a net carbon uptake by using inventory method. Besides the overall increasing trends, both the VCI and the VHI showed decreasing trends in eastern Inner Mongolia, Yangtze River delta and Pearl River Delta, indicating an increasing constraints of vegetation growth in these regions. The vegetation growth in Yangtze River Delta and Pearl River Delta could be reduced by increasing urban land development in past decades (He et al., 2014). In addition, the vegetation stress in eastern Inner Mongolia could be associated with the raised temperature in this period (Fig. 11). These results are in accordance with the findings of the NDVI analysis reported by Piao et al. (2015).

However, the regions with increasing vegetation stress from the VHI were even wider than the VCI (Figs. 9b and 10b). This was especially in the northern China and in the eastern Qinghai-Tibetan Plateau. This divergence could be associated with the introduction of bright temperature into the VHI. The vegetation stress from the VHI could be more precise in the condition of the negative-correlation between the VCI and temperature in the northern China. However, the vegetation stress in eastern Qinghai-Tibetan Plateau could be overestimated by the VHI in comparison with the VCI. Namely, the correlations between the VCI and temperature were positive in this region, indicating an enhanced vegetation growth on the condition of climate warming (Figs. 7 and 11).

5. Conclusions

The NOAA developed a dataset entitled the Vegetation Health Product (VHP), including VCI, TCI and VHI products (Kogan et al., 2011). While the VCI and the VHI were widely employed, performances of the two indices were analyzed and compared to monitor the dynamics of vegetation activity. Furthermore, the vegetation activity in response to weather-related drivers in China were assessed by using the

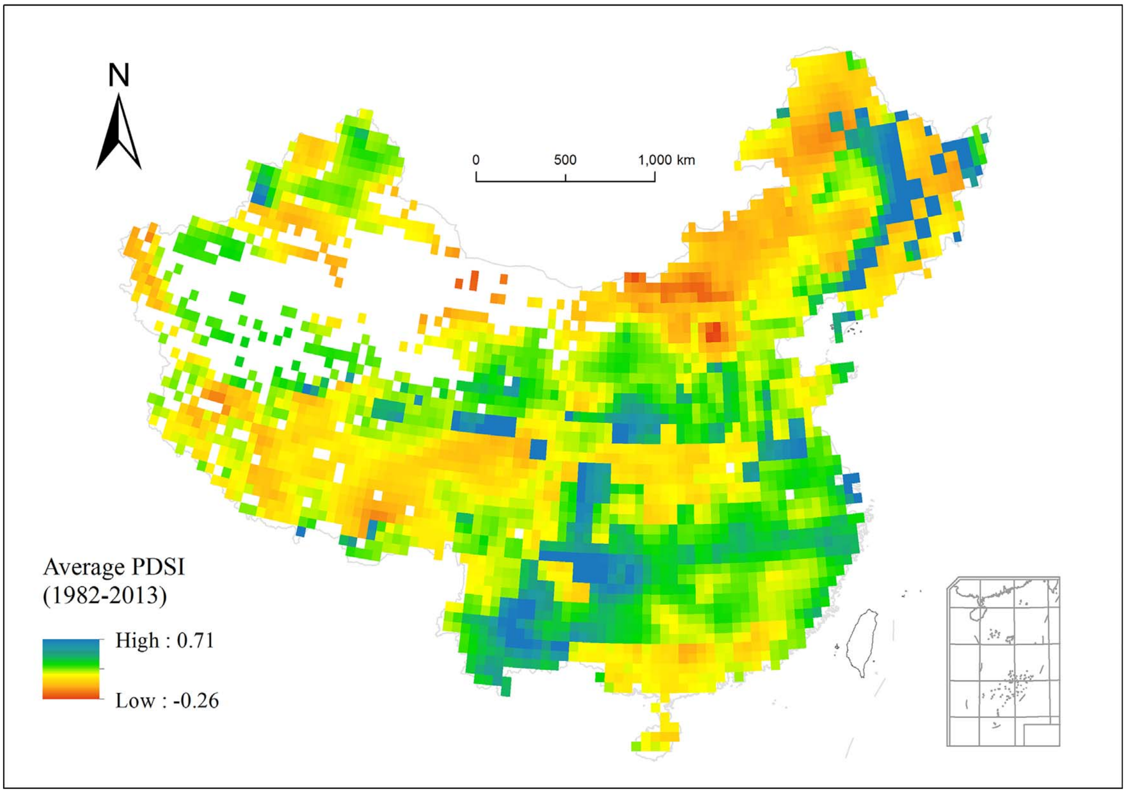

Fig. 8. Average PDSI from 1982 to 2013 in China.

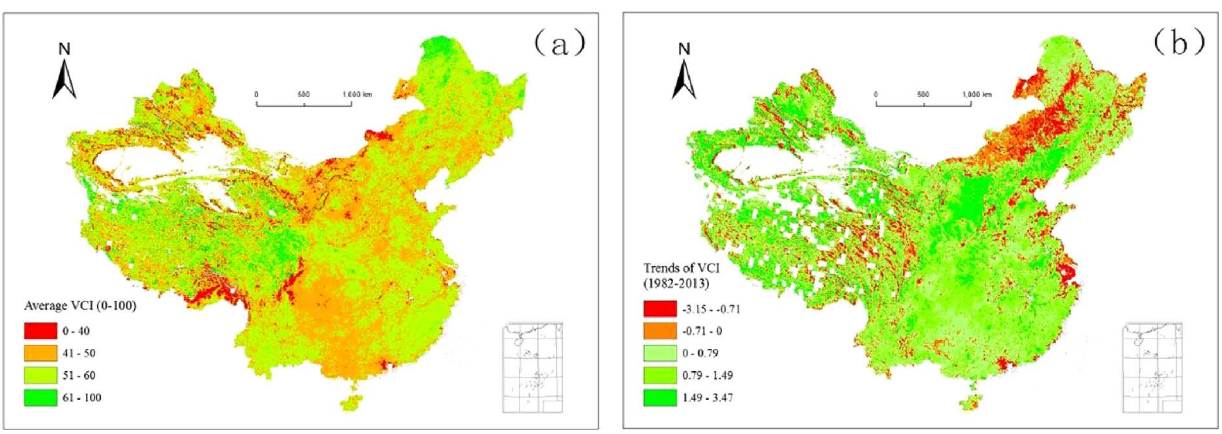

Fig. 9. Average values and trends of the VCI during 1982–2013 in China (a) average VCI during 1982–2013, (b) linear trends of the VCI.

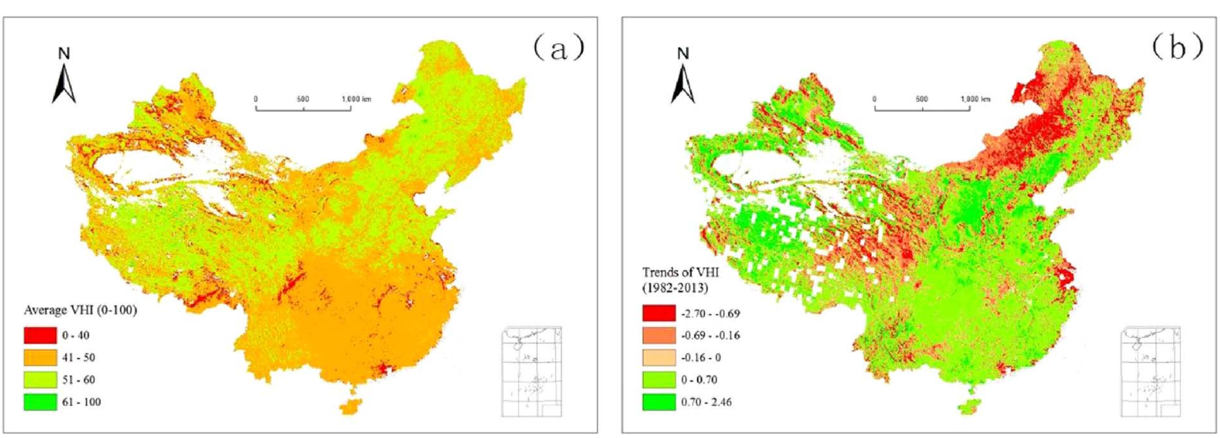

Fig. 10. The same details as Fig. 9, but for the VHI.

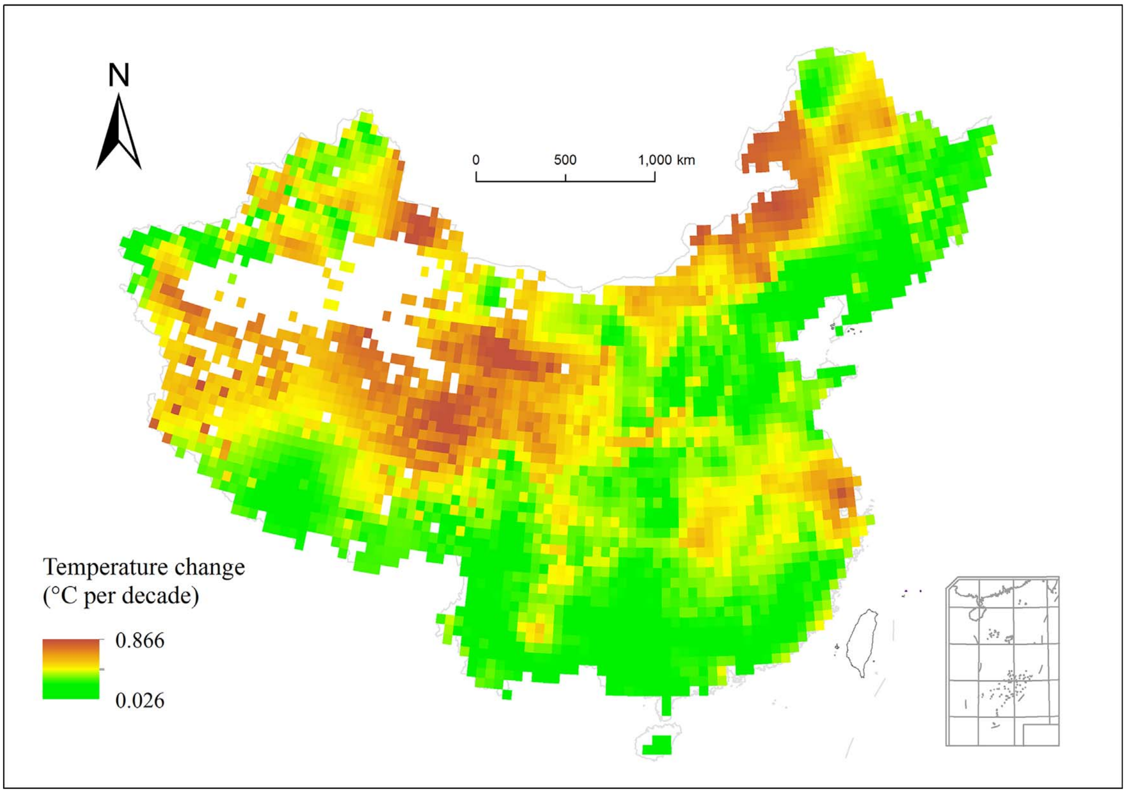

Fig. 11. Spatial pattern of temperature trends in China from 1982 to 2013.

VCI and the VHI as a surrogate, respectively.

We found that both the VCI and the VHI showed widely-distributed vegetation stress for a long period (about two months) in past decades, and enhancing trend of vegetation activity in China. However, correlations between the VCI and temperature can be changeable for complex topography, climate conditions and vegetation types in China. For instances, negative correlations could be obvious in semi-arid and subhumid climatic regions in northern China (e.g., eastern Inner Mongolia). However, correlation between vegetation growth and temperature was found to be positive in humid regions (e.g., in southern China) and in the eastern Qinghai-Tibetan Plateau with high elevations. In addition, the VCI could be available when detecting the vegetation activity in comparison with the VHI, especially in humid regions (e.g., southern China) and the regions with high elevations (e.g., Qinghai-Tibetan Plateau). This phenomena could be associated with the assumption of the VHI that warming temperature can act negatively on vegetation vigour and therefore cause stress to the vegetation growth (Karnieli et al., 2006). Consequently, vegetation activity could be enhanced in the condition of climate warming in such regions. We propose that the VCI and the VHI should be used cautiously in the context of climate warming. In future studies, the VCI and the VHI should be well improved to fit different topography and climate condition for widely use in different vegetation distributions.

Acknowledgements

The authors would like to thank anonymous reviewers for the insightful and constructive comments. This work was supported by the National Natural Science Foundation of China (Grant No. 41401438) and the Project Funded by the Priority Academic Program Development of Jiangsu Higher Education Institutions.

References

Bala, G., et al., 2007. Combined climate and carbon-cycle effects of large-scale deforestation. Proc. Natl. Acad. Sci. 104 (16), 6550–6555.
Bhuiyan, C., Singh, R.P., Kogan, F.N., 2006. Monitoring drought dynamics in the Aravalli region (India) using different indices based on ground and remote sensing data. Int. J. Appl. Earth Obs. Geoinf. 8 (4), 289–302.
Challinor, A.J., et al., 2014. A meta-analysis of crop yield under climate change and adaptation. Nat. Clim. Change 4, 287–291.
Chen, X., Pan, W., 2002. Relationships among phenological growing season, time-integrated normalized difference vegetation index and climate forcing in the temperate region of eastern China. Int. J. Climatol. 22 (14), 1781–1792.
Committee on Natural Division Sciences, 1959. Climatic Regionalization of China. Science Press, Beijing.
Dai, A., Trenberth, K.E., Qian, T., 2004. A global data set of palmer drought severity index for 1870–2002: relationship with soil moisture and effects of surface warming. J. Hydrometeorol. 5 (6), 1117–1130.
de Jong, R., de Bruin, S., de Wit, A., Schaepman, M.E., Dent, D.L., 2011. Analysis of monotonic greening and browning trends from global NDVI time-series. Remote Sens. Environ. 115 (2), 692–702.
Fang, J., Piao, S., He, J., Ma, W., 2004. Increasing terrestrial vegetation activity in China, 1982–1999. Sci. China Ser. C: Life Sci. 47 (3), 229–240.
He, C., Liu, Z., Tian, J., Ma, Q., 2014. Urban expansion dynamics and natural habitat loss in China: a multiscale landscape perspective. Glob. Change Biol. 20 (9), 2886–2902.
Hong, Y., Nix, H.A., Hutchinson, M.F., Booth, T.H., 2005. Spatial interpolation of monthly mean climate data for China. Int. J. Climatol. 25 (10), 1369–1379.
Huang, B.W., 1958. A preliminary scheme for comprehensive physical regionalization in China. Acta Geographica Sinica 24 (4), 348–365.
Hutchinson, M.F., 1998. Interpolation of rainfall data with thin plate smoothing splines. Part II: analysis of topographic dependence. J. Geogr. Inf. Decis. Anal. 2 (2), 152–167.
Ji, L., Peters, A.J., 2003. Assessing vegetation response to drought in the northern Great Plains using vegetation and drought indices. Remote Sens. Environ. 87 (1), 85–98.
Karnieli, A., et al., 2006. Comments on the use of the vegetation health index over Mongolia. Int. J. Remote Sens. 27 (10), 2017–2024.
Karnieli, A., et al., 2010. Use of NDVI and land surface temperature for drought assessment: merits and limitations. J. Clim. 23 (3), 618–633.
Kogan, F., Sullivan, J., 1993. Development of global drought-watch system using NOAA/AVHRR data. Adv. Space Res. 13 (5), 219–222.
Kogan, F., Yang, B., Wei, G., Zhiyuan, P., Xianfeng, J., 2005. Modelling corn production in China using AVHRR-based vegetation health indices. Int. J. Remote Sens. 26 (11), 2325–2336.
Kogan, F., Vargas, M., Ding, H., Guo, W., 2011. VHP Algorithm Theoretical Basis Document.

Kogan, F.N., 1990. Remote sensing of weather impacts on vegetation in non-homogeneous areas. Int. J. Remote Sens. 11 (8), 1405–1419.
Kogan, F.N., 1995. Application of vegetation index and brightness temperature for drought detection. Adv. Space Res. 15 (11), 91–100.
Kogan, F.N., 1997. Global drought watch from space. Bull. Am. Meteorol. Soc. 78 (4), 621–636.
Komuscu, A.U., 1999. Using the SPI to Analyze Spatial and Temporal Patterns of Drought in Turkey.
Lü, Y., et al., 2015. Recent ecological transitions in China: greening, browning, and influential factors. Sci. Rep. 5.
Linderholm, H.W., 2006. Growing season changes in the last century. Agric. For. Meteorol. 137 (1–2), 1–14.
Liu, S., Gong, P., 2012. Change of surface cover greenness in China between 2000 and 2010. Chin. Sci. Bull. 57 (22), 2835–2845.
Liu, B., Henderson, M., Zhang, Y., Xu, M., 2010. Spatiotemporal change in China's climatic growing season: 1955–2000. Clim. Change 99 (1–2), 93–118.
Menzel, A., Jakobi, G., Ahas, R., Scheifinger, H., Estrella, N., 2003. Variations of the climatological growing season (1951–2000) in Germany compared with other countries. Int. J. Climatol. 23 (7), 793–812.
Orlovsky L., Kogan F., Eshed E., Dugarjav C., 2011. Monitoring Droughts and Pastures Productivity in Mongolia Using NOAA-AVHRR Data. In: F. Kogan, A. Powell, O. Fedorov (F. Kogan, A. Powell and O. Fedorov)ˆ(F. Kogan, A. Powell and O. Fedorovs)|,*Use of Satellite and In-Situ Data to Improve Sustainability. Springer Netherlands, pp. 69–79.
Pei, F., Li, X., Liu, X., Lao, C., 2013a. Assessing the impacts of droughts on net primary productivity in China. J. Environ. Manage. 114 (0), 362–371.
Pei, F., Li, X., Liu, X., Wang, S., He, Z., 2013b. Assessing the differences in net primary productivity between pre- and post-urban land development in China. Agric. For. Meteorol. 171–172 (0), 174–186.
Peng, S., et al., 2011. Recent change of vegetation growth trend in China. Environ. Res. Lett. 6 (4), 044027.
Peng, S., et al., 2014. Afforestation in China cools local land surface temperature. Proc. Natl. Acad. Sci. 111 (8), 2915–2919.
Piao, S., et al., 2009. The carbon balance of terrestrial ecosystems in China. Nature 458 (7241), 1009–1013.
Piao, S., et al., 2011. Changes in satellite-derived vegetation growth trend in temperate and boreal Eurasia from 1982 to 2006. Glob. Change Biol. 17 (10), 3228–3239.
Piao, S., et al., 2012. Impacts of climate and CO2 changes on the vegetation growth and carbon balance of Qinghai–Tibetan grasslands over the past five decades. Glob. Planet. Change 98, 73–80.
Piao, S., et al., 2014. Evidence for a weakening relationship between interannual temperature variability and northern vegetation activity. Nat. Commun. 5.
Piao, S., et al., 2015. Detection and attribution of vegetation greening trend in China over the last 30 years. Glob. Change Biol. 21 (4), 1601–1609.
Seiler, R.A., Kogan, F., Sullivan, J., 1998. AVHRR-based vegetation and temperature condition indices for drought detection in Argentina. Adv. Space Res. 21 (3), 481–484.
Solomon, S., et al., 2007. Climate Change 2007: the Physical Science Basis. Contribution of Working Group I to the Fourth Assessment Report. Cambridge University Press, Cambridge, United Kingdom and New York, NY, USA 996 pp.
Song, Y., Linderholm, H.W., Chen, D., Walther, A., 2010. Trends of the thermal growing season in China, 1951–2007. Int. J. Climatol. 30 (1), 33–43.
Szép, I.J., Mika, J., Dunkel, Z., 2005. Palmer drought severity index as soil moisture indicator: physical interpretation, statistical behaviour and relation to global climate. Phys. Chem. Earth Parts A/b/c 30 (1), 231–243.
Trenberth, K.E., et al., 2014. Global warming and changes in drought. Nat. Clim. Change 4 (1), 17–22.
Ulanova, E., 1975. Climate and Winter Wheat Yield. pp. 298.
Unganai, L.S., Kogan, F.N., 1998. Drought monitoring and corn yield estimation in Southern Africa from AVHRR data. Remote Sens. Environ. 63 (3), 219–232.
Walther, G.R., et al., 2002. Ecological responses to recent climate change. Nature 416 (6879), 389.
Wang, Z., Zhai, P., Zhang, H., 2003. Variation of drought over northern China during 1950–2000. J. Geog. Sci. 13 (4), 480–487.
Xiao, J., Moody, A., 2004. Trends in vegetation activity and their climatic correlates: China 1982–1998. Int. J. Remote Sens. 25 (24), 5669–5689.
Zhai, P., et al., 1999. Changes of climate extremes in China. Clim. Change 42 (1), 203–218.
Zhao, M., Running, S.W., 2010. Drought-induced reduction in global terrestrial net primary production from 2000 through 2009. Science 329 (5994), 940–943.
Zou, X., Zhai, P., Zhang, Q., 2005. Variations in droughts over China: 1951–2003. Geophys. Res. Lett. 32 (4), L04707.